Reactive photoinduced species in estuarine waters. Characterization of hydroxyl radical, singlet oxygen and dissolved organic matter triplet state in natural oxidation processes

Reactive photoinduced species in estuarine waters. Characterization of hydroxyl radical, singlet oxygen and dissolved organic matter triplet state in natural oxidation processes

Fadi al Housari,[a] Davide Vione,[b] Serge Chiron,[a] Stéphane Barbati*[a]

Received (in XXX, XXX) Xth XXXXXXXXX 200X, Accepted Xth XXXXXXXXX 200X
First published on the web Xth XXXXXXXXX 200X
DOI: 10.1039/b000000x

This paper describes the reactive photo-induced species (RPS) hydroxyl radical ($HO^\bullet$), singlet oxygen ($^1O_2$) and chromophoric dissolved organic matter triplet state (^{3}CDOM*) comparatively in fresh water (Canal) and estuarine water (Vaccarès), sampled in the Camargue region, southern France. Experiments were conducted with a medium-pressure Hg lamp in a glass photoreactor (λ >290 nm, 220 $W \cdot m^{-2}$ irradiance between 290 and 400 nm). Steady-state concentration and initial production rate of RPS were determined for $HO^\bullet$ and for $^1O_2$. $HO^\bullet$ and $^1O_2$ were indirectly identified in the presence of benzene and furfuryl alcohol, respectively, as specific probes. The steady-state measured concentration [$HO^\bullet$] was $(1.72\pm0.01)\times10^{-16}$ M and $(9.41\pm0.12)\times10^{-17}$ M for Vaccarès and Canal waters samples, respectively, and the respective [$^1O_2$] was $(2.06\pm0.22)\times10^{-13}$ M and $(5.44\pm0.04)\times10^{-14}$ M. The interference of ^{3}CDOM* or other species in the determination of $^1O_2$ with furfuryl alcohol, and of $^1O_2$ in the quantification of ^{3}CDOM* with 2,4,6-trimethylphenol was also quantitatively assessed. We developed here a kinetic model underlying that the solar photo-transformation of xenobiotic organic compounds is induced by the three different photooxidants $HO^\bullet$, $^1O_2$ and ^{3}CDOM*.

Introduction

Aqueous photochemistry is an important process for the transformation of endogenous and exogenous organic components in natural waters. Under solar irradiation, photochemical transformations in aquifers, defined here as Natural Oxidation Processes (NOP), involve direct and indirect photochemical reactions. In direct photolysis, organic compounds absorb radiation themselves and undergo chemical changes. In indirect photochemical pathways, chromophoric dissolved organic matter (CDOM), nitrate, nitrite and Fe(III) act as sensitizers by absorbing radiation, then inducing indirect degradation of surrounding organic compounds. Several important intermediates play a key role in the photodegradation pathways, including the reactive photoinduced species (RPS) $HO^\bullet$, $^1O_2$, $ROO^\bullet$, $HOO^\bullet$, $O_2^{\bullet-}$, $CO_3^{\bullet-}$, $NO_2^\bullet$, e_{aq}^-, and ^{3}CDOM*.[1,2] Particularly, $HO^\bullet$, $^1O_2$ and ^{3}CDOM* are of prime importance for their contribution to organic fate in sunlit aquifers.[3] Hydroxyl radical is one of the most reactive free radicals reacting at nearly diffusion-controlled rate,[4] and which is also involved in the mineralization of organic compounds. In advanced oxidation processes (AOPs), $HO^\bullet$ has a central role, following the definition by Glaze:[5] AOPs are near-ambient temperature and pressure water treatment processes that involve the generation of $HO^\bullet$ in sufficient quantity to affect water purification. In sunlit natural water, $HO^\bullet$ is mainly produced by the photolytic reactions involving NO_2^-, NO_3^-,[6] and irradiated CDOM.[7-9] Additionally, Fe(III) has also been reported to enhance $HO^\bullet$ production via the photo-Fenton reaction,[10,11] or from the photoreduction of Fe(III) hydroxocomplexes.[12,13] The photoproduction rate of $HO^\bullet$ in many river waters and seawaters has been determined to be in the order $6\text{-}150\times10^{-12}$ $M \cdot s^{-1}$ and $4\text{-}50\times10^{-12}$ $M \cdot s^{-1}$, respectively.[14] It is noteworthy that $HO^\bullet$ is also efficiently consumed by natural dissolved organic matter, which limits its steady-state concentration in waters illuminated by sunlight.[3] CDOM is known to promote organic pollutant degradation in sunlight[8] via its excited triplet states, which induce electron transfer with organic compounds, or via singlet oxygen ($^1\Delta_g$) produced from energy tranfer of ^{3}CDOM* to molecular oxygen.[8,15] Photochemical processes are strongly related to the chemical composition of water, because of the possible reaction between RPS and intrinsic components of natural water.[3,16] A major parameter in natural water is the concentration of chloride that distinguishes marine water from fresh water. The oceans, covering 71% of the Earth's surface, form a significant reservoir and reaction medium for exogenous contaminants, particularly in the coastal water. In estuarine areas, the ionic composition of river water is strongly modified by chloride enrichment due to the seawater proximity. Chloride may affect the photochemistry of exogenous organics and lead to the production of chloroderivatives.[17] Additionally, it has been reported that estuarine waters contain higher DOM comparatively to river water.[18] To our best knowledge the RPS $HO^\bullet$, $^1O_2$ and ^{3}CDOM* have never been studied and identified at the same time in freshwater samples and *a fortiori* in estuarine waters.

The aim of this study was then to quantify the primary RPS in estuarine waters and to determine their production kinetics in real samples in order to bring a comprehensive method to model photochemical reactions in natural waters characterized

by high salinity and high DOM . The specific probes benzene, furfuryl alcohol and 2,4,6-trimethylphenol (TMP) were used to characterize the reactive species $HO^{\bullet}$, $^1O_2$ and the triplet states of CDOM, respectively.

Experimental

Chemicals

All reagents and chemicals were purchased commercially from the following suppliers: 2,4,6-trimethylphenol (TMP) and furfuryl alcohol (FFA) (98%) from Alfa Aesar, NaN_3 (99%), methanol and acetonitrile, from Sigma-Aldrich, isopropanol from Carlo Erba. All chemicals and reagents were used without further purification. All glassware and plastic were acid washed with HCl (5%) and rinsed with distilled water followed by Milli-Q water prior to use. HPLC eluents were prepared with Milli-Q water.

Water samples

Two sampling sites from Camargue (Vaccarès, Canal) were adopted, taking water from about 15 cm below the surface. Water was then filtered through 0.45 μm pore-size membranes, and stored at 4°C in the dark until analysis. Storage and all measurements were performed at the natural water pH. Sample analysis is presented in Table 1. Spectra were recorded in a cell with 1 cm optical path lengh. UV-Vis spectra of the samples are presented on Fig. 1. It is noticeable that the Vaccarès sample shows a much higher absorption than the Canal one. It can be attributed to the higher organic matter content of the Vaccarès sample (see Table 1) for wavelength values down to 230-240 nm, where CDOM dominates the absorption.[7,9] Interestingly, the absorbance ratio of the two samples is much higher than the NPOC ratio. This implies that the specific absorbance of CDOM is higher in the case of Vaccarès. Below 230 nm other water components would also play a very important role (*e.g.* nitrate, nitrite and Fe species).[6,7,9] Nitrate and nitrite cannot account for the difference as they are more concentrated in the case of Canal. In contrast, the higher Fe concentration of the Vaccarès sample could play a role below 230 nm.

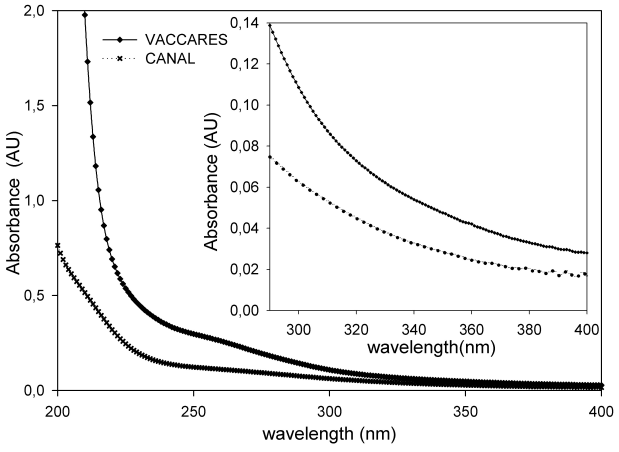

Fig. 1 UV-Vis spectra for Canal and Vaccarès water samples collected on April 28, 2008.

Table 1 Physical and chemical parameters of water samples. Error intervals represent μ±σ.

Sample	Canal	Vaccarès
Sampling date:	28 April 2008	28 April 2008
Cl^-, M	$(1.18 \pm 0.03) \times 10^{-3}$	$(1.90 \pm 0.05) \times 10^{-1}$
NO_3^-, M	$(4.36 \pm 0.03) \times 10^{-5}$	$(1.64 \pm 0.01) \times 10^{-5}$
NO_2^-, M	$(9.57 \pm 0.05) \times 10^{-7}$	$(8.26 \pm 0.05) \times 10^{-7}$
Fe, ppb	3.81±0.90	22.81±3.06
NPOC, mg C/L^{-1}	19.83 ± 0.30	32.11 ± 0.60
pH	7.81	8.01
Conductivity, mS	0.62	36.50
Salinity, g/L	0.10	26.20
$r_{HO^{\bullet}}$, $M \cdot s^{-1}$	$(1.52\pm0.01)\times10^{-11}$	$(1.93\pm0.01)\times10^{-11}$
$[HO^{\bullet}]_{ss}$, M	$(9.41\pm0.12)\times10^{-17}$	$(1.72\pm0.01)\times10^{-16}$
$\sum_i k_i [S_i]$, s^{-1}	$(1.62\pm0.03)\times10^{5}$	$(1.12\pm0.01)\times10^{5}$
$r_{^1O_2}$, $M \cdot s^{-1}$	$(1.36\pm0.01)\times10^{-8}$	$(5.14\pm0.54)\times10^{-8}$
$[^1O_2]_{ss}$, M	$(5.44\pm0.04)\times10^{-14}$	$(2.06\pm0.22)\times10^{-13}$

Irradiation experiments

Stationary photolysis experiments were carried out in a cylindrical immersion-type glass photoreactor (0.5 L – Heraeus TQ 150 Model) equipped with a water-cooled medium-pressure Hg lamp (glass cut off (λ < 290 nm), maximum emission wavelengths at 313, 366, 406, 436, 546 and 578 nm). The incident, volumetric photon flux in solution was 1.0×10^{-4} einstein L^{-1} s^{-1}. The irradiance between 290 and 400 nm was around 220 W m^{-2}. The radiation path length inside the reactor was 2 cm. The whole assembly was wrapped with aluminum foil. Upon irradiation, aliquots were removed at various time intervals and analyzed by HPLC-UV. Each experiment was carried out in triplicate.

Analytical determinations

pH was measured by pH meter ORION model 420A. The measures of iron were performed by ICP-AES with a JY2000 ULTRACE apparatus (Jobin Yvon Horiba). ICP-AES conditions: Plasma Argon flow: 12 L/min, Plasma power: 1000W, Nebulisation pressure 3.2 bars. The standard solutions were supplied by Aldrich (concentration of metal 1000 mg/L in acidified solution containing 1% HNO_3). The identification of Fe was performed at 260 nm. UV-Vis absorption spectra of water samples were recorded using a spectrophotometer model Agilent 8453 and ChemStation software (quartz cells, 1 cm path length). Anions (NO_3^-, NO_2^-, Cl^-) were analyzed with a DIONEX ICS 3000 Ion chromatograph, equipped with an Autosampler AS 40, a gradient pump, a Dionex Ion Pac AS11-HC 4×250mm anion exchange column, a Dionex IonPac AG 11-HC 4×5mm guard column, a ASRS-ULTRA 300-4 mm suppressor, and two detectors: Ultimate 3000 Photodiode Array Detector UV/VIS and conductimetric one at 35°C. The eluents were H_2O and 100 mM NaOH. Flow rate was 1.5 $mL \cdot min^{-1}$. Elution Gradient: 0-16 min (NaOH 1.3% / H_2O 98.7%); 16-29 min (from NaOH 1.3% to NaOH 60%).The retention times were (min): Cl^- (13.64), NO_3^- (21.8). NO_2^- concentration was

measured by sulfanilamide method.[19]

Organic carbon was quantified as non-purgeable organic carbon (NPOC) with 5050A/SSM 5000 Shimadzu carbon analyzer, after acidification of the sample with concentrated $HClO_4$ and a 20 min air purge to eliminate CO_2. Three measures were systematically acquired for each experiment, and averaged to give the final value. HPLC analysis was carried out by a Hitachi HPLC chromatograph equipped with a L-2400 UV detector and using a RP-C18 LiChrospher column (Merck, length 250 mm, diameter 4.6 mm, particle size 5 µm). Samples were eluted with a mixture of acetonitrile (ACN) and water acidified with orthophosphoric acid (0.1%) at a flow rate of 0.8 mL·min^{-1}. The percentage volume of ACN/acidified water was 20:80 and 60:40 for FFA and TMP, respectively. Retention times (min)/detection wavelength (nm) were: FFA (7.06/218), 6-hydroxy(2H)pyran-3(6H)-one (Pyranone) (4.30/218), TMP (9.97/205). Benzene consumption and phenol formation were monitored with the same HPLC apparatus. Samples were eluted with a 40:60 mixture of ACN/water. Retention times (min)/detection wavelength (nm) were: phenol (4.62/ 210), benzene (9.50/210).

Methodology

The adopted methology was to measure HO$^\bullet$ with the formation of phenol from benzene as a probe reaction (95% yield),[9,14] $^1O_2$ upon transformation of FFA plus control experiments (quenching with azide),[15] and ^{3}DOM* with the phototransformation of TMP.[8] The errors associated to the relevant quantities (±σ) were derived from the goodness of the fit of the theoretical kinetic functions to the experimental data or, where relevant, from the rules of error propagation.

Results and discussion

Measurement of hydroxyl radical

Hydroxyl radicals were identified and quantified in natural water samples with the benzene probe as described by Vione *et al*.[9] Benzene was chosen as a model compound for examining indirect photolysis due to its fast reaction with HO$^\bullet$ (second-order rate constant 7.8×10^9 M^{-1}·s^{-1})[4] and to its lack of reactivity by direct photolysis. The transformation reaction of benzene to phenol was monitored as a function of time assuming that phenol was produced only upon reaction between benzene and HO$^\bullet$ (95% yield). This hypothesis is justified by the fact that natural waters afford limited interference on this reaction by other reactive transients.[20] Applying the steady-state approximation to [HO$^\bullet$] the rate of benzene reaction is given by:

$$\frac{d[Phenol]}{dt} = k_B \cdot [HO^\bullet] \cdot [Benzene] = \frac{k'_B \cdot r_{HO^\bullet} \cdot [Benzene]}{\sum_i k_i \cdot [S_i] + k_B \cdot [Benzene]} \quad (1)$$

Where k_B is the second-order rate constant for the reaction between benzene and HO$^\bullet$ (7.8×10^9 M^{-1}·s^{-1}), and $k'_B = 0.95 \cdot k_B$. S_i is a generic HO$^\bullet$ scavenger present in the natural water sample, having rate constant k_i for reaction with HO$^\bullet$. $r_{HO^\bullet}$ is the rate of HO$^\bullet$ photoformation. The reaction of phenol with HO$^\bullet$ was not considered because only the initial rates were taken into account. Eq. 1 was resolved for low concentration of benzene to determine [HO$^\bullet$] (denominator becoming equal to $\sum_i k_{S_i} \cdot [S_i]$ by neglecting the reaction of benzene with HO$^\bullet$ compared to the reaction of S_i with HO$^\bullet$) and at high concentration of benzene to determine $r_{HO^\bullet}$ (denominator equal to k_B [Benzene] by neglecting the reaction of S_i with HO$^\bullet$ compared to the reaction of benzene with HO$^\bullet$). The time evolution of phenol upon irradiation of the two natural water samples in the presence of benzene at different initial concentrations is shown in Fig. 2. The initial formation rate of phenol was calculated as the slope of the tangent at *t=0* to the curve fitting the experimental concentration values of phenol. Following the procedure of Vione et al.,[9] [HO$^\bullet$] was determined from the tangent at *t=0* to the curve representing the initial formation rate of phenol as a function of [Benzene] (Fig. 3). The values of $r_{HO^\bullet}$, [HO$^\bullet$] and $\sum_i k_{S_i} \cdot [S_i]$ are reported in Table 1. The associated errors are referred to the goodness of the fit of the theoretical curves (Eq. 1) to the experimental data shown in Fig. 3.

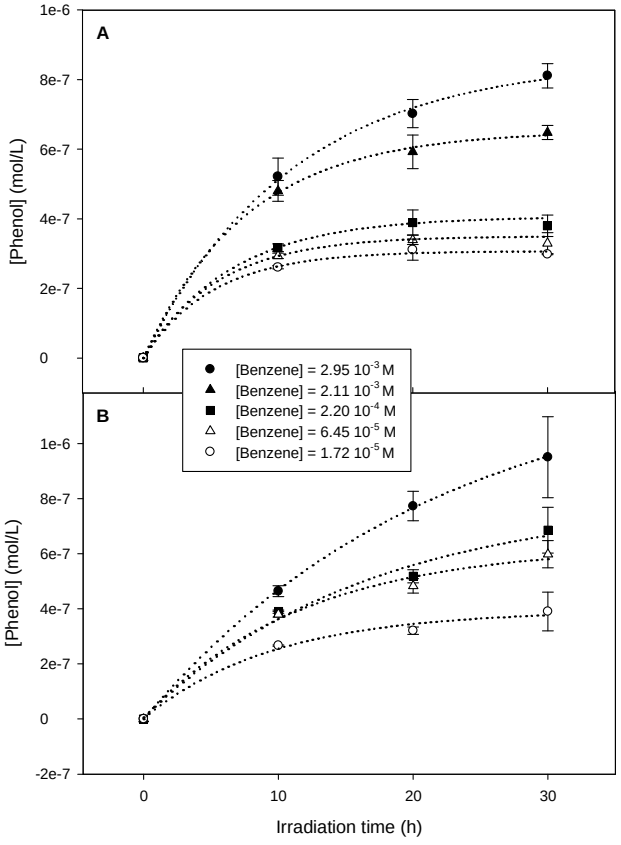

Fig. 2 Time evolution of phenol upon irradiation of water from A) Vaccarès and B) Canal for different concentration values of benzene. SD is given for tree replicates.

The adopted procedure is based on the hypothesis of a selective reaction of HO$^\bullet$ with benzene. Phenol could also be produced from alternative sources like $^1O_2$ and humic acids via the triplet state ^{3}CDOM*. However, $^1O_2$ is little reactive toward benzene,[21] and the addition of HO$^\bullet$ scavengers in excess is able to completely quench the formation of phenol

from benzene upon irradiation of humic acids or lake water.[20] The deduced steady-state [HO•] in the Vaccarès water sample ((1.72±0.01)×10^{-16} M) was about 1.8 times higher than that of Canal ((9.41±0.12)×10^{-17} M). The overall scavenging rate constant ($\sum_i k_{S_i} \cdot [S_i]$) values were (1.12±0.01)×10^5 and (1.62±0.03)×10^5 s^{-1} for the Vaccarès and Canal water samples, respectively (Table 1).

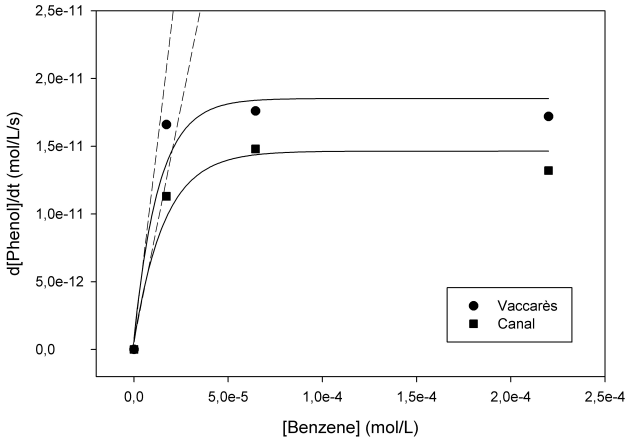

Fig. 3 Comparative initial formation rate of phenol upon irradiation of water from Vaccarès and Canal, as a function of the initial benzene concentration. The tangents representing the $lim_{[Benzene]\rightarrow 0}\{d[Phenol]/dt \cdot [Benzene]^{-1}\}$ give access to [HO•]

Dissolved organic matter is most likely the main scavenger of HO• in the two samples. In contrast, chloride even at elevated concentration is extremely unlikely to be a significant HO• scavenger at neutral to basic pH. While significant consumption of hydroxyl radicals by Cl^- is operational under acidic conditions, no scavenging could be detected at circumneutral pH, in the presence of chloride at concentration up to at least 1 M.[9,17] Interestingly, the lower scavenging rate constant of the Vaccarès sample in the presence of higher NPOC suggests that the Vaccarès organic matter is considerably less reactive toward HO• than the Canal one.

Also interesting is the higher $r_{HO\bullet}$ in the case of Vaccarès. Among the possible HO• sources, nitrate is much more concentrated in Canal, and the concentration of nitrite is similar in the two samples but slightly higher for Canal. Moreover, note that $[NO_3^-]\cdot[NO_2^-]^{-1}$ is < 100 in both cases, which suggests a more important role of nitrite as HO• source compared to nitrate.[6] Of the other possible species that could be involved in the photoinduced generation of HO•, CDOM and Fe are more concentrated in the Vaccarès sample. The two compounds together could be involved into photo-Fenton reactions, which would therefore be presumably more important in the estuarine sample. However, it should be pointed out that the photo-Fenton process is for instance the prevailing HO• source in the Satilla river (USA), characterized by high Fe levels (5-14 µM) and relatively acidic pH (< 7).[22] In the present case, even in the Vaccarès sample the concentration of Fe is sub-µM and the pH is quite high. Under basic conditions the generation of HO• by the Fenton reaction is inhibited,[23] for which reason the Vaccarès sample could hardly be considered as an ideal system for the photo-Fenton process to be an important source of HO•. Additionally, the generation rate of HO• upon direct irradiation of Fe(III) species under neutral to basic conditions is quite low.[24] Another possibility is that the high generation rate of HO• in the Vaccarès sample is due to the presence of more concentrated and more active CDOM (see Figure 1 and Table 1), which could produce hydroxyl radicals directly upon irradiation.[9]

Involvement of singlet oxygen ($^1O_2$)

Under solar irradiation, natural waters are known to produce hydroxyl radical and singlet oxygen. Consequently, these reactive species should be involved in the transformation pathways of organic compounds (R) that are present in water. The relevant processes are described in Eqs. 2-3, where P_1 and P_2 are the photoproducts of the reaction of R with HO• and $^1O_2$, respectively. The reactivity of the organic compound R with RPS may be affected by various scavengers present in the natural water matrix ($S_{i,j}$), which can compete with R for the reaction with the photogenerated transients (Eqs. 4-5). The equations representing the oxidation rate of R (r_R) and the reaction rates of HO• ($r_{HO\bullet}$) and $^1O_2$ ($r_{^1O_2}$) are given by Eqs. 7-9, where k_1 is the second-order rate constant of the reaction of R with HO•, k_2 that with $^1O_2$, k_i and k_j the second-order rate constants of the reaction of the scavenger S_i and S_j with HO• and $^1O_2$, respectively. Finally, k_d is the first-order rate constant for the deactivation of $^1O_2$ in water (2.5×10^5 s^{-1}).[25]

$$R + HO^\bullet \xrightarrow{k_1} P_1 \quad (2)$$

$$R + {}^1O_2 \xrightarrow{k_2} P_2 \quad (3)$$

$$S_i + HO^\bullet \xrightarrow{k_i} P_i \quad (4)$$

$$S_j + {}^1O_2 \xrightarrow{k_j} P_j \quad (5)$$

$${}^1O_2 \xrightarrow{k_d} O_2 \quad (6)$$

$$r_R = -\frac{d[R]}{dt} = k_1[R][HO^\bullet] + k_2[R][{}^1O_2] \quad (7)$$

$$r_{HO\bullet} = \left(k_1[R] + \sum_i k_i[S_i]\right)[HO^\bullet] \quad (8)$$

$$r_{^1O_2} = \left(k_2[R] + k_d + \sum_j k_j[S_j]\right)[{}^1O_2] \quad (9)$$

Note that under the steady-state conditions that are operational for HO• and $^1O_2$ in surface waters, $r_{HO\bullet}$ and $r_{^1O_2}$ would also represent the formation rates of the relevant species under irradiation.

The characterisation of $^1O_2$ was carried out with furfuryl alcohol (FFA), which is known to react with singlet oxygen (k_2 = 1.2×10^8 M$^{-1}\cdot$s^{-1}) to give the corresponding 6-hydroxy(2H)pyran-3(6H)-one (pyranone) in 85% yield.[15] The initial rate of FFA photooxydation (r_{FFA}) was measured for several initial FFA concentrations. Assuming that FFA reacts with both hydroxyl radical and singlet oxygen, r_{FFA} can be

expressed as follows (note that R = FFA in Eqs. 2-3):

$$r_{FFA} = \frac{r_{HO^\bullet} \cdot k_1 \cdot [FFA]}{\sum_i k_i \cdot [S_i] + k_1 \cdot [FFA]} + \frac{r_{^1O_2} \cdot k_2 \cdot [FFA]}{\sum_j k_j \cdot [S_j] + k_2 \cdot [FFA] + k_d} \quad (10)$$

In this equation, the fitting variables are $r_{^1O_2}$ and $\Sigma_j\, k_j\, [S_j]$. The variables $r_{HO^\bullet}$ and $\Sigma_i\, k_i\, [S_i]$ were deduced from the measurement of $HO^\bullet$ in the presence of benzene (see above). The preliminary fit of the experimental data with Eq. 10 (data not shown) yielded $\Sigma_j\, k_j\, [S_j] \ll k_2\, [FFA] + k_d$, which suggests that the term $\Sigma_j\, k_j\, [S_j]$ can be neglected.

The irradiation of FFA (10^{-4} M) in natural waters indicated that FFA depletion reached 44.5% and 21.1% after 240 min for the Vaccarès and Canal water samples, respectively (Fig. 4). Only a small percentage of FFA reacted under irradiation, comparatively to Richard and co-workers who obtained 80% FFA removal in similar conditions after 200 min of irradiation in laboratory-grade water in the presence of fulvic acid.[15]

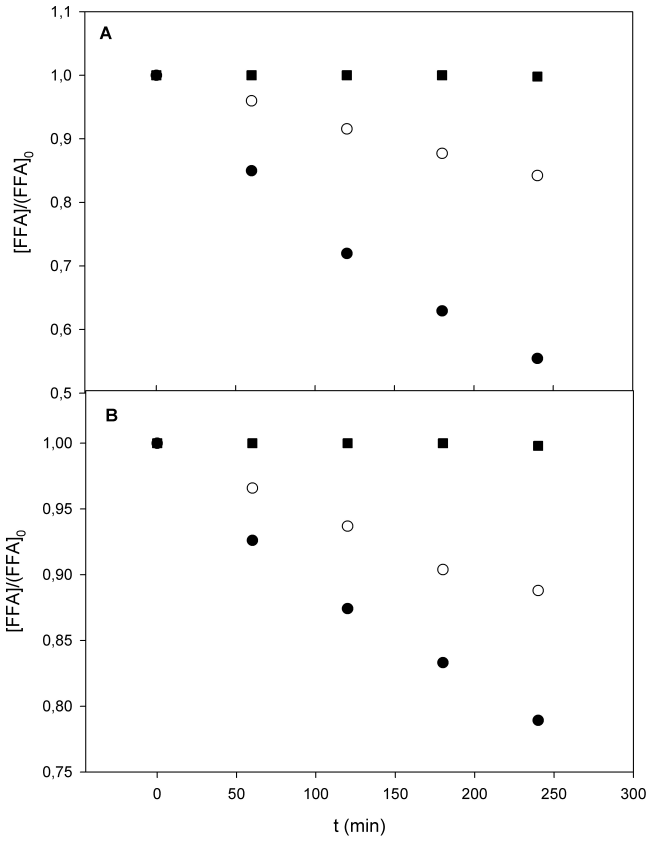

Fig. 4. Normalized evolution of FFA vs. time under polychromatic light in A) Vaccarès water and B) Canal water. (■) FFA (0.25×10^{-4} M) in milliQ water, (●) FFA (0.25×10^{-4} M) in real water; (○) FFA (0.25×10^{-4} M) in real water + sodium azide (3×10^{-3} M).

The low degradation yields observed here could be explained by the lower photochemical reactivity of whole CDOM samples compared to fulvic acids, or by the matrix effect of the natural waters because of the presence of dissolved antioxidants.[26] The control of the reaction in milliQ water indicated that FFA did no undergo direct phototransformation under irradiation. The effect of the azide anion (3×10^{-3} M) is also reported in Fig. 4. Azide is known to react with $HO^\bullet$ and $^1O_2$, with second-order rate constants $k_3 = 1.4\times10^{10}\ M^{-1}\cdot s^{-1}$ [27] and $k_4 = 7.8\times10^{8}\ M^{-1}\cdot s^{-1}$ [28] respectively. In the presence of the azide, Eq. (10) would be modified as follows:

$$r_{FFA} = \frac{r_{HO^\bullet} \cdot k_1 \cdot [FFA]}{\sum_i k_i \cdot [S_i] + k_1 \cdot [FFA] + k_3 \cdot [N_3^-]} + \frac{r_{^1O_2} \cdot k_2 \cdot [FFA]}{\sum_j k_j \cdot [S_j] + k_2 \cdot [FFA] + k_d + k_4 \cdot [N_3^-]} \quad (11)$$

Eq. (11) foresees a 90% inhibition of FFA degradation in the presence of 3 mM N_3^-, but the experimental data (Fig. 4) show that the decrease of FFA was only partially inhibited for both the Vaccarès (65%) and the Canal sample (47%). These results indicate that [FFA] continued decreasing, albeit to a reduced extent, when $^1O_2$ and $HO^\bullet$ were quenched by azide. The oxidation of N_3^- in the studied system is expected to produce the azide radical $N_3^\bullet$, which shows significant reactivity toward many substituted phenols. Interestingly, no reactivity data of $N_3^\bullet$ with FFA or other alcohols are reported,[29] which suggests that $N_3^\bullet$ would not be involved to a significant extent in the transformation of FFA. It is therefore hypothesized that additional reactive species, possibly ^{3}CDOM* or organic matter-derived radicals (e.g. $RO^\bullet$ and/or $ROO^\bullet$),[3] could be involved in FFA depletion upon irradiation of natural water.

The next paragraph discusses in greater detail the hypothesis that the residual transformation of FFA in the presence of the azide is due to the reaction with ^{3}CDOM*, or other species generated upon irradiation and transformation of organic matter.

Involvement of species derived from dissolved organic matter in the transformation of FFA

If the degradation of FFA is carried out by ^{3}CDOM*, the process would take place according to the following Eqs. 12-15:[30,31]

$$\text{CDOM} + h\nu \rightarrow {}^3\text{CDOM}^* \qquad [r_{3CDOM^*}] \quad (12)$$

$${}^3\text{CDOM}^* \rightarrow \text{CDOM} \qquad [k^*] \quad (13)$$

$${}^3\text{CDOM}^* + \text{FFA} \rightarrow \text{Products} \qquad [k_5] \quad (14)$$

$${}^3\text{CDOM}^* + O_2 \rightarrow \text{CDOM} + {}^1O_2 \qquad [k_6] \quad (15)$$

The chemistry of species such as $RO^\bullet$ and/or $ROO^\bullet$ is not known in sufficient detail to enable the setting up of a similar reaction scheme, but equivalent reactions could possibly be operational.

The role of the interfering species has been approximately assessed from the difference (r_{DIFF}) between the experimental (Table 2) and the calculated (Eq. 11) FFA rates in the presence of the azide. It was possible to obtain that $r_{DIFF} = 7\times10^{-6}\cdot[FFA]$ for Canal and $r_{DIFF} = 3\times10^{-6}\cdot[FFA]$ for Vaccarès.

Under the hypothesis that the difference between the experimental and the calculated values is due to ^{3}CDOM*,

and applying the steady-state approximation to [^{3}CDOM*], an exact expression for r_{DIFF} would be:

$$r_{DIFF} = \frac{r_{^3CDOM^*} \cdot k_5 \cdot [FFA]}{k_5 \cdot [FFA] + k_6 \cdot [O_2] + k^*} \quad (16)$$

Where r_{3CDOM*} and k* are the formation rate of ^{3}CDOM* and the deactivation rate constant of ^{3}CDOM*, respectively. It would also be k_5·[FFA] « k_6·[O_2] + k*.[30] Considering that the involvement of ^{3}CDOM* is not demonstrated, Eq. 16 can be more generically written as $r_{DIFF} = \alpha\,[FFA]$ (α *unit in* s^{-1}). The rate data of FFA without sodium azide would then be given by the sum of the contributions of HO$^\bullet$, $^1O_2$, and ^{3}CDOM* or other species. The following, simplified fitting function was obtained:

$$r_{FFA} = \frac{r_{HO^\bullet} \cdot k_1 \cdot [FFA]}{\sum_i k_i \cdot [S_i] + k_1 \cdot [FFA]} + \frac{r_{^1O_2} \cdot k_2 \cdot [FFA]}{k_2 \cdot [FFA] + k_d} + \alpha \cdot [FFA] \quad (17)$$

considering that $\sum_j k_{Sj} \cdot [S_j]$ « k_d.[31,32] From the experimental data of r_{DIFF} one gets $\alpha = 7\times10^{-6}$ for Canal and 3×10^{-6} for Vaccarès. The Fig. 5 reports the experimental rates of r_{FFA} vs. [FFA] for the natural waters Canal and Vaccarès (solid squares). The dashed lines represent the fit with Eq. 17, where $r_{^1O_2}$ was the only fit variable. Consecutively, it was found $r_{^1O_2}$ = (1.36±0.01)×10^{-8} M·s^{-1} and (5.14±0.54)×10^{-8} M·s^{-1} for Canal and Vaccarès, respectively. The errors represent the goodness of the fit of Eq. 17 to the experimental data. The dotted line indicates what would be the model without taking into account the contribution of ^{3}CDOM* or other interfering species (α *[FFA]* term in Eq. 17). It is apparent that the contribution of the interfering agents is much more important in the case of Canal, for which the value of α was more than double compared to Vaccarès. The fact that r_{1O2} is higher for Vaccarès compared to Canal is consistent with the higher NPOC (see Table 1) and even more with the higher content of CDOM (see Fig. 1) of Vaccarès. Indeed, $^1O_2$ is produced by the excited triplet states ^{3}CDOM* (reaction 15). It is also possible to derive the steady-state [$^1O_2$] in the absence of FFA or the azide. Consider Eq. 9 with [R] = 0 and $\sum_j k_{Sj} \cdot [S_j]$ « k_d,[31,32] from which one gets $[^1O_2] = r_{^1O_2}\, k_d^{-1}$. The steady-state [$^1O_2$] values thus derived are reported in Table 1.

Table 2. Experimental rate of FFA phototransformation in the absence (r_{FFA}) and in the presence (r_{FFAq}) of sodium azide (3×10^{-3} M), in the Canal and Vaccarès water samples.

[FFA] / 10^6 M	Canal		Vaccarès	
	r_{FFA} / 10^{-10} M.s^{-1}	r_{FFAq} / 10^{-10} M.s^{-1}	r_{FFA} / 10^{-10} M.s^{-1}	r_{FFAq} / 10^{-10} M.s^{-1}
25	4.0	2.1	10.3	2.9
50	8.2	4.5	19.0	3.9
100	15.8	8.1	36.5	6.4
200	24.3	4.8	46.9	8.7

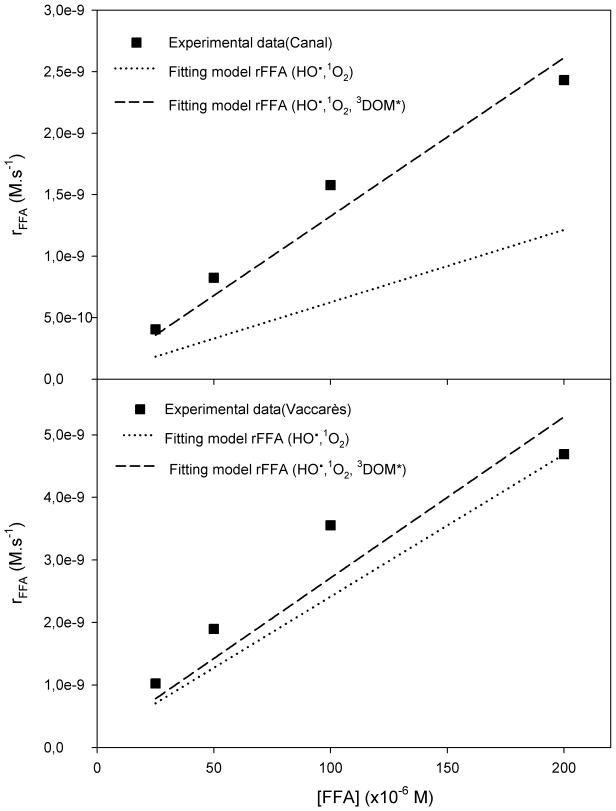

Fig. 5 Fitting model of r_{FFA} taking in account the three RPS in A) Canal and B) Vaccarès water samples. FFA concentrations: 0.25, 5.0, 1.0 and 2.0×10^{-4} M.

Quantitation of ^{3}CDOM*

2,4,6-Trimethylphenol (TMP) has successfully been used to probe the photosensitising properties of natural waters. This electron-rich phenol is readily transformed upon irradiation in the presence of chromophoric dissolved organic matter or humic substances.[30,33] TMP can react with singlet oxygen (k_2 = 6.3×10^7 M^{-1}·s^{-1}),[34] triplet states or other radicals (*e.g.* HO$^\bullet$). However, it has been reported that the rate of TMP phototransformation in the presence of humic or fulvic acids was not affected by the presence of the azide, confirming the negligible involvement of $^1O_2$ under such conditions.[35] The formation of ^{3}CDOM* was specifically determined from the irradiation of TMP in Vaccarès and Canal water samples. Fig.6 reports the transformation rate of TMP at different initial concentrations upon irradiation of the natural water samples. The transformation rate r_{TMP} can be written as follows:

$$-\frac{d[TMP]}{dt} = \frac{r_{^3CDOM^*} \cdot k_{TMP}[TMP]}{k_{TMP}[TMP] + k_6[O_2] + k^*} + \frac{r_{^1O_2} \cdot k_2 \cdot [TMP]}{k_2[TMP] + k_d} \quad (18)$$

The reaction rate constant of TMP with hydroxyl radicals was neglected, based on previous findings that k_1·[HO$^\bullet$] « k_{TMP} [^{3}CDOM*] in natural waters,[30] where k_{TMP} is the second-order reaction rate constant between TMP and ^{3}CDOM*.

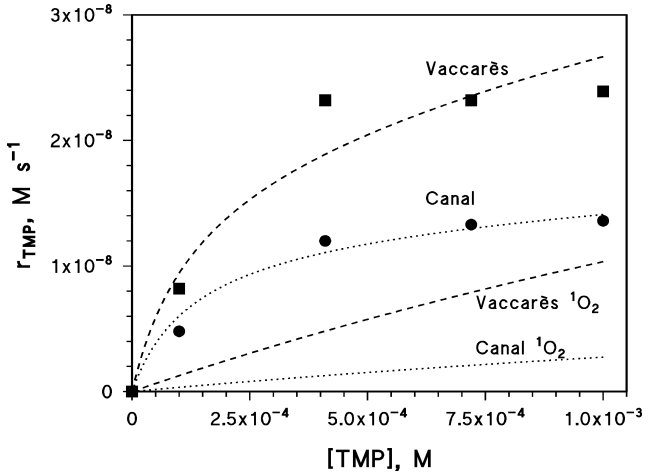

Fig.6 Plot of r_{TMP} vs. [TMP] for Canal and Vaccarès water samples. Experimental data and fitting curves.

The fit of the experimental data was carried out with Eq. 18, with $k_2 = 6.3\times10^7$ $M^{-1}\cdot s^{-1}$, $k_d = 2.5\times10^5$ s^{-1}, $k_6\cdot[O_2] + k^* = 5\times10^5$ s^{-1},[25] $r_{^1O_2} = (1.36\pm0.01)\times10^{-8}$ $M\cdot s^{-1}$ and $(5.14\pm0.54)\times10^{-8}$ $M\cdot s^{-1}$ for Canal and Vaccarès, respectively, and r_{3CDOM*} and k_{TMP} as fit variables. The fit yielded $r_{3CDOM*} = (1.8\pm0.3)\times10^{-8}$ $M\cdot s^{-1}$ and $k_{TMP} = (4.8\pm4.4)\times10^9$ $M^{-1}\cdot s^{-1}$ for Vaccarès, $r_{3CDOM*} = (1.4\pm0.1)\times10^{-8}$ $M\cdot s^{-1}$ and $k_{TMP} = (3.0\pm1.1)\times10^9$ $M^{-1}\cdot s^{-1}$ for Canal. Fig. 6 also reports the calculated contribution of $^1O_2$ to the transformation of TMP in the two samples, which is definitely not negligible in the case of Vaccarès. It is noticeable the elevated error on k_{TMP} in the case of the Vaccarès sample. However, a further fit carried out on the same data by taking fixed $k_{TMP} = 3.0\times10^9$ $M^{-1}\cdot s^{-1}$ as for Canal yielded a very similar $r_{3CDOM*} = 1.9\times10^{-8}$ $M\cdot s^{-1}$. The determination of r_{3CDOM*} from the Vaccarès data can therefore be considered as sufficiently robust.

Interestingly, in the case of Canal it is $r_{3CDOM*} \approx r_{^1O_2}$, which is reasonable because ^{3}CDOM* is the main source of $^1O_2$ in surface waters.[15,30] However, for the Vaccarès sample one finds $r_{3CDOM*} < r_{^1O_2}$. Possible explanations are: *(i)* the addition of the azide to the Vaccarès sample was able to quench both $^1O_2$ and some of the interfering species. The role of these species would be underestimated from the azide data and, as a consequence, one would overestimate $r_{^1O_2}$. *(ii)* TMP was not able to react with the whole of ^{3}CDOM* in the Vaccarès sample, possibly because some transients would preferentially react with O_2 to yield $^1O_2$, even with TMP in large excess. One should assume that such peculiar transients are particularly common in the estuarine sample. *(iii)* The adopted literature value of k_d is too elevated. Note that the model fit to the data of Fig. 5 would be largely improved by adopting a lower value of k_d. In that case $r_{^1O_2}$ would be considerably lower. Interestingly, in cases *(i)* and *(ii)* one has to assume a rather peculiar behavior of the estuarine sample.

Expected transformation kinetics of model substrates

The data obtained or available for $HO^\bullet$ ($r_{HO\bullet}$ and $\Sigma_i k_i [S_i]$), $^1O_2$ (r_{1O2} and k_d) and ^{3}CDOM* (r_{3CDOM*} and $k_6 [O_2] + k^*$) can be used for the assessment of the transformation kinetics of model substrates in the two water samples under the adopted irradiation conditions. It would therefore be possible to compare the relative importance of the different transformation pathways. Unfortunately, while a wide data set is available for the reactivity of the dissolved molecules with $HO^\bullet$, that with ^{3}CDOM* has been studied for relatively few compounds (mainly phenylurea herbicides and sulphonamides),[8] for which additionally there is no data concerning the (presumably low, however) reaction rate constant with $^1O_2$. Table 3 reports the reaction rate constants with $HO^\bullet$ of two amino acids (tyrosine and histidine), 4-chlorophenol (4CP) and the corresponding phenolate ($4CP^-$), and the phenylurea herbicides diuron and fenuron.[4,36,37] For phenylureas the reaction rate constants with ^{3}CDOM* are also reported,[38] while for the other compounds the rate constants with $^1O_2$ only are available.[36,39]

Let R be a generic compound dissolved in water. Under reasonable pseudo-first order conditions, the half life time of R for reaction with $HO^\bullet$, $^1O_2$ and ^{3}CDOM*, respectively, is expressed by:

$$t_{1/2}^{R,OH^\bullet} = \frac{\ln 2 \cdot \sum_i k_i \cdot [S_i]}{k_{R,OH^\bullet} \cdot r_{OH^\bullet}} \qquad (19)$$

$$t_{1/2}^{R,^1O_2} = \frac{\ln 2 \cdot k_d}{k_{R,^1O_2} \cdot r_{^1O_2}} \qquad (20)$$

$$t_{1/2}^{R,^3CDOM*} = \frac{\ln 2 \cdot (k_6 \cdot [O_2] + k^*)}{k_{R,^3CDOM*} \cdot r_{^3CDOM*}} \qquad (21)$$

where $k_d = 2.5\cdot10^5$ s^{-1},[21] and $k_6 [O_2] + k^* = 5\cdot10^5$ s^{-1}.[25] The values of $r_{OH\bullet}$, $\Sigma_i k_i [S_i]$, $r_{^1O_2}$ ~~and r_{3CDOM*}~~ for the Vaccarès and Canal samples are reported in Table 1, together with the associated errors. The values of the reaction rate constants of the different model compounds (substrates) with the transient species $HO^\bullet$, $^1O_2$ and ^{3}CDOM*, and the corresponding half-life times of the substrates are reported in Table 3. They are expressed in hours of continuous irradiation under the adopted device. The UV irradiance was 220 W m^{-2}, namely around 7 times more intense than the irradiance of sunlight at noon during the summer solstice at mid latitude.[40] Also note that the errors associated to the half-life times have been derived by error propagation, from the relevant quantities reported in Table 1, and rounded to the precision of the $t_{½}$ values.

In the case of $k_{R,3CDOM*}$, the main problem is that CDOM is not a species of definite chemical composition. Accordingly, the relevant reaction rate constants can only be measured relative to model molecules that are representative of the nature of CDOM. It has been reported that 3'-methoxyacetophenone (MAP) and benzophenone (BP) can be used to this purpose.[38] The reactivity of the relevant excited triplet states toward fenuron and diuron is quite different, with MAP being considerably less reactive than BP. For this reason Table 3 reports an interval for the values of k_{3CDOM*}, with the upper end corresponding to k_{3BP*} and the lower end to k_{3MAP*}.

Table 3. Rate constants for the reaction of some model substrates with $HO^{\bullet}$, $^1O_2$, and $^3CDOM^*$.[36-39] The interval in the case of $^3CDOM^*$ shows the different reactivity of $^3BP^*$ and $^3MAP^*$ with diuron and fenuron. The corresponding values of $t_{½}$ for the Vaccarès(V) and Canal (C) samples are based on the reported literature rate constants, the results of the irradiation experiments carried out in this work, and the equations (19)-(21). The values of $t_{½}$ are expressed in hours of continuous irradiation under the adopted device. n/a = not available.

	Tyrosine	Histidine	4-CP	4-CP$^-$	Diuron	Fenuron
$k_{\bullet OH}$, M^{-1} s^{-1}	$1.3\cdot10^{10}$	$5.0\cdot10^{9}$	$7.6\cdot10^{9}$	$4.1\cdot10^{9}$	$5\cdot10^{9}$	$7\cdot10^{9}$
$k_{^1O_2}$, M^{-1} s^{-1}	$9.0\cdot10^{6}$	$6.6\cdot10^{7}$	$6.0\cdot10^{6}$	$1.9\cdot10^{8}$	n/a	n/a
$k_{^3CDOM^*}$, M^{-1} s^{-1}	n/a	n/a	n/a	n/a	$(9\div520)\cdot10^{6}$	$(8.1\div200)\cdot10^{7}$
$t_{½}^{\bullet OH}$(C), h	160±5	410±10	270±10	500±15	410±10	290±10
$t_{½}^{^1O_2}$(C), h	390±5	54±1	590±10	19±1	n/a	n/a
$t_{½}^{^3CDOM^*}$(C), h	n/a	n/a	n/a	n/a	13÷760	3.4÷85
$t_{½}^{\bullet OH}$(V), h	90±1	220±2	150±1	270±3	220±2	160±2
$t_{½}^{^1O_2}$(V), h	100±10	14±1	160±20	4.9±0.5	n/a	n/a
$t_{½}^{^3CDOM^*}$(V), h	n/a	n/a	n/a	n/a	10÷590	2.7÷66

From the $t_{½}$ data reported in Table 3 it is apparent that, first of all, the photochemical reactivity of the Vaccarès (estuarine, brackish) sample is higher compared to Canal (freshwater). The difference is highest for the reaction with $^1O_2$, and lowest for $^3CDOM^*$. It is remarkable that the estuarine sample is photochemically more reactive than the riverine/freshwater one. The most plausible explanation is the higher occurrence and reactivity of CDOM in the studied estuarine sample, which in the case of the Rhône river would be combined with a delta where the water is quite shallow. Higher intrinsic photoreactivity and shallow water would combine together in producing a delta environment where photochemical processes could play a very important role, also considering that such an environment is located in the Mediterranean region where sunlight is abundant. Such a result strengthens the previous findings that the Rhône delta is a very useful field photochemical reactor, where for instance the photoinduced nitration processes can be easily detected.[41]

As far as the relative reactivity with $HO^{\bullet}$ and $^1O_2$ is concerned, in both samples tyrosine and 4CP are expected to react faster with the hydroxyl radical, histidine and the 4-chlorophenolate with singlet oxygen. In the case of the compounds that react faster with $HO^{\bullet}$, the reactivity with $^1O_2$ is of secondary importance but it is not negligible. In contrast, for the molecules that react faster with $^1O_2$, the reaction with $HO^{\bullet}$ is unimportant. Note that $4CP^-$, in analogy with many chlorophenolates, would also undergo direct photolysis to a significant extent.[36,42-44]

In the case of the two phenylurea pesticides chosen as model substrates, the comparison of the reactivity with $HO^{\bullet}$ and with $^3CDOM^*$ should take into account the relatively large interval of $t_{½}^{^3CDOM^*}$. Such an interval depends on the choice of BP and MAP as model molecules for CDOM. By comparison with $t_{½}^{HO^{\bullet}}$ one gets that, in the case of diuron, the reaction with the hydroxyl radical is more important if the reactivity of $^3CDOM^*$ is more similar to that of $^3MAP^*$, while $^3CDOM^*$ is a more significant sink if its reactivity resembles that of $^3BP^*$. In case the reaction with $HO^{\bullet}$ is more important, it would be around twice as fast as that with $^3CDOM^*$. In the opposite case, the reaction with $^3CDOM^*$ could out-compete that of $HO^{\bullet}$ by an order of magnitude or more.

In the case of fenuron the reaction with $^3CDOM^*$ is expected to be more important compared to $HO^{\bullet}$, irrespective of the hypothesized reactivity of $^3CDOM^*$ ($^3BP^*$-like or $^3MAP^*$-like). Accordingly, the present results confirm the findings of Canonica and coworkers that $^3CDOM^*$ is a very important sink of phenylurea herbicides in surface water.[8] However, under definite circumstances of CDOM photoreactivity and with certain substrates (e.g. diuron), the reaction with $HO^{\bullet}$ cannot be neglected as a sink.

Conclusions

In this study, for the first time to our knowledge, the photochemical formation of $HO^{\bullet}$, $^1O_2$ and $^3CDOM^*$ was determined in both a freshwater and an estuarine environment (Canal and Vaccarés samples, respectively). The estuarine sample contained more organic matter as measured by NPOC, as expected, but interestingly the organic matter of the estuarine sample also showed a higher intrinsic absorption of radiation. As a consequence, the absorbance ratio between the estuarine and the freshwater sample is higher than the ratio of NPOC, which could make the CDOM in the estuarine sample considerably more photoreactive.

The reported CDOM features in the two samples are reflected in the respective photochemical activity as measured by the formation of $HO^{\bullet}$, $^1O_2$, and $^3CDOM^*$. The formation rates of all these species are considerably higher in the estuarine sample, where the indirect photolysis of organic contaminants could therefore be faster. Such a finding is somewhat expected in the case of $^1O_2$ and $^3CDOM^*$ that are produced by irradiated colored organic matter. The radical $HO^{\bullet}$ is also produced by nitrate and nitrite, which have equal to higher concentration in the freshwater sample. It can therefore be inferred that the higher photoproduction of $HO^{\bullet}$ in the estuarine sample can be accounted for by irradiated CDOM. Overall, the transition from the Rhône freshwater to the delta results into more favorable conditions for photochemistry, because of the combination of higher intrinsic reactivity, shallower water columns and longer residence time of water.[41]

In this work it was also shown that the quantification of $^1O_2$ through the degradation of FFA suffers from some interference by $^3CDOM^*$ or other species such as $ROO^{\bullet}$ and/or $RO^{\bullet}$. At the same time, the determination of $^3CDOM^*$ using TMP resents of the interference by $^1O_2$. However, it was possible to overcome the problem upon addition of NaN_3 to the FFA system, which allowed for the quantification of the contribution of the interfering species to the degradation of

FFA. In a similar way, $^1O_2$ is able to react with TMP and therefore to interfere with the determination of ^{3}CDOM*. The knowledge of the formation rate of $^1O_2$ allows its inclusion into the kinetic model that describes the degradation of TMP, and the measurement of the formation rate of ^{3}CDOM* is therefore possible despite the interference. Interestingly, Fig. 6 shows that the reaction rate between TMP and $^1O_2$ increases linearly with [TMP], while the total transformation rate of TMP (r_{TMP}) has a less-than-linear increase with [TMP]. The consequence is that the interference by the reaction between TMP and $^1O_2$ becomes more important at elevated [TMP].

The procedure depicted in the present paper (measurement of $^1O_2$ with FFA, of other interfering species with FFA + NaN_3, and inclusion of $^1O_2$ into the kinetic model of TMP degradation to exactly quantify ^{3}CDOM*) could therefore be useful for future studies into the quantification of $^1O_2$ and ^{3}CDOM* upon irradiation of surface waters.

Acknowledgements

DV acknowledges financial support by the Italian Inter-University Consortium of Chemistry and the Environment (INCA) and Università di Torino – Ricerca locale.

Notes and references

[a] *Laboratoire de Chimie Provence - UMR 6264, Équipe Chimie de l'Environnement Continental - Aix-Marseille Université - 3, Place Victor Hugo (Case 29) - 13331 Marseille Cedex 3, France. Fax: +33 4 91 10 63 77 ; Tel: +33 4 91 10 65 66; E-mail: fadihousari@voila.fr, serge.chiron@univ-provence.fr, stephane.barbati@univ-provence.fr*

[b] *Dipartimento di Chimica Analitica, Università di Torino, Via P. Giuria 5, 10125 Torino, Italy. Fax: +39 0116707615; Tel: +39 0116707874; E-mail: davide.vione@unito.it*

Notes and references

1 S. S. Walse, S. L. Morgan, L. Kong and J. L. Ferry, Role of dissolved organic matter, nitrate, and bicarbonate in the photolysis of aqueous fipronil, *Environ. Sci Technol.*, 2004, **38**, 3908-3915.

2 R. Huie and P. Neta, Kinetics of one-electron transfer-reactions involving ClO_2 and NO_2, *J. Phys. Chem.*, 1986, **90**, 1193-1198.

3 C. Richard and S. Canonica, Aquatic phototransformation of organic contaminants induced by coloured dissolved natural organic matter, *Handb. Environ. Chem.*, 2005, 299-323.

4 G. Buxton, C. Greenstock, W. Helman and A. Ross, Critical-review of rate constants for reactions of hydrated electrons, hydrogen-atoms and hydroxyl radicals ($^{\bullet}$OH/$^{\bullet}O^-$) in aqueous-solution, *J. Phys. Chem. Ref. Data*, 1988, **17**, 513-886.

5 W. Glaze, J. Kang and D. Chapin, The chemistry of water-treatment processes involving ozone, hydrogen-peroxide and ultraviolet-radiation, *Ozone Sci. Eng.*, 1987, **9**, 335-352.

6 C. Minero, S. Chiron, G. Falletti, V. Maurino, E. Pelizzetti, R. Ajassa, M. E. Carlotti and D. Vione, Photochemical processes involving nitrite in surface water samples, *Aquatic Sci.*, 2007, **69**, 71-85.

7 P. Vaughan and N. Blough, Photochemical formation of hydroxyl radical by constituents of natural waters, *Environ. Sci. Technol.*, 1998, **32**, 2947-2953.

8 S. Canonica, Oxidation of aquatic organic contaminants induced by excited triplet states, *Chimia*, 2007, **61**, 641-644.

9 D. Vione, G. Falletti, V. Maurino, C. Minero, E. Pelizzetti, M. Malandrino, R. Ajassa, R. Olariu and C. Arsene, Sources and sinks of hydroxyl radicals upon irradiation of natural water samples, *Environ. Sci. Technol.*, 2006, **40**, 3775-3781.

10 B. Voelker and B. Sulzberger, Effects of fulvic acid on Fe(II) oxidation by hydrogen peroxide, *Environ. Sci. Technol.*, 1996, **30**, 1106-1114.

11 B. Voelker, F. Morel and B. Sulzberger, Iron redox cycling in surface waters: effects of humic substances and light, *Environ. Sci. Technol.*, 1997, **31**, 1004-1011.

12 I. Pozdnyakov, Y. Sosedova, V. Plyusnin, V. Grivin, D. Vorob'ev and N. Bazhin, Optical spectra and kinetic characteristics of radicals formed upon the photolysis of aqueous solutions of a $FeOH_{aq}^{2+}$ complex and phenol, *Russ. Chem. Bull.*, 2004, **53**, 2715-2722.

13 I. Pozdnyakov, Y. Sosedova, V. Plyusnin, E. Glebov, V. Grivin, D. Vorobyev and N. Bazhin, Photodegradation of organic pollutants in aqueous solutions caused by $Fe(OH)_{aq}^{2+}$ photolysis: Evidence of OH radical formation, *Int. J. Photoenergy*, 2004, **6**, 89-93.

14 K. Takeda, H. Takedoi, S. Yamaji, K. Ohta and H. Sakugawa, Determination of hydroxyl radical photoproduction rates in natural waters, *Anal. Sci.*, 2004, **20**, 153-158.

15 S. Halladja, A. Ter Halle, J. P. Aguer, A. Boulkamh and C. Richard, Inhihition of humic substances mediated photooxygenation of furfuryl alcohol by 2,4,6-trimethylphenol. Evidence for reactivity of the phenol with humic triplet excited states, *Environ. Sci.Technol.*, 2007, **41**, 6066-6073.

16 S. Canonica and P. G. Tratnyek, Quantitative structure-activity relationships for oxidation reactions of organic chemicals in water, *Environ. Toxicol.Chem.*, 2003, **22**, 1743-1754.

17 S. Chiron, C. Minero and D. Vione, Photodegradation processes of the Antiepileptic drug carbamazepine, relevant to estuarine waters, *Environ. Sci. Technol.*, 2006, **40**, 5977-5983.

18 S. Mylon, K. Chen and M. Elimelech, Influence of natural organic matter and ionic composition on the kinetics and structure of hematite colloid aggregation: Implications to iron depletion in estuaries, *Langmuir*, 2004, **20**, 9000-9006.

19 J. Rodier, in *L'analyse de l'eau, eaux naturelles, eaux résiduaires, eau de* mer, Dunod, Paris, 7th edition, 1984, p. 1365.

20 D. Vione, V. Lauri, C. Minero, V. Maurino, M. Malandrino, M. E. Carlotti, R. I.Olariu and C. Arsene, Photostability and photolability of dissolved organic matter upon irradiation of natural water samples under simulated sunlight, *Aquat. Sci.*, 2009, **71**, 34-45.

21 S. H. Chien, M. F. Cheng, K. C. Lau and W. K. Li, Theoretical study of the Diels-Alder reactions between singlet ($^1\Delta_g$) oxygen and acenes, *J. Phys. Chem. A*, 2005, **109**, 7509-7518.

22 E. M. White, P. P. Vaughan and R. G. Zepp, Role of the photo-Fenton reaction in the production of hydroxyl radicals and photobleaching of colored dissolved organic matter in a coastal river of the southeastern United States, *Aquat. Sci*,. 2003, **65**, 402-414.

23 S. J. Hug and O. Leupin, Iron-catalyzed oxidation of arsenic(III) by oxygen and by hydrogen peroxide: pH-dependent formation of oxidants in the Fenton reaction, *Environ. Sci. Technol.*, 2003, **37**, 2734-2742.

24 S. Chiron, S. Barbati, S. Khanra, B. K. Dutta, M. Minella, C. Minero, V. Maurino, E. Pelizzetti and D. Vione, Bicarbonate-enhanced transformatino of phenol upon irradiation of hematite, nitrate and nitrite, *Photochem. Photobiol. Sci*,. 2009, **8**, 91-100.

25 M. A. J. Rodgers and P. T. Snowden, Lifetime of O_2 ($^1\Delta_g$) in liquid water as determined by time-resolved infrared luminescence measurements, *J. Am. Chem. Soc.* 1982, **104**, 5541-5543.

26 S. Canonica and H. U. Laubscher. Inhibitory effect of dissolved organic matter on triplet-induced oxidation of aquatic contaminants, *Photochem. Photobiol. Sci.*, 2008, **7**, 547-551.

27 N. Motohashi and Y. Saito, competitive measurement of rate constants for hydroxyl radical reactions using radiolytic hydroxylation of benzoate, *Chem. Pharm. Bull.* 1993, **41**, 1842-1845.

28 F. Wilkinson and J. Brummer, Rate constants for the decay and reactions of the lowest electronically excited singlet-state of molecular-oxygen in solution, *J. Phys. Chem. Ref. Data*, 1981, **10**, 809-1000.

29 P. Neta, R. E. Huie and A. B. Ross, Rate constants for reactions of inorganic radicals in aqueous solution, *J. Phys. Chem. Ref. Data*, 1988, **17**, 1027-1230.

30 S. Canonica and M. Freiburghaus, Electron-rich phenols for probing the photochemical reactivity of freshwaters, *Environ. Sci. Technol.*, 2001, **35**, 690-695.
31 J. Hoigné, Formulation and calibration of environmental reaction kinetics: Oxidations by aqueous photooxidants as an example. In *Aquatic Chemical Kinetics*. Ed. W. Stumm , Wiley, NY, 1990, pp. 43-70.
32 D. Vione, D. Bagnus, V. Maurino and C. Minero. Quantification of singlet oxygen and hydroxyl radicals upon UV irradiation of surface water, *Environ. Chem. Lett.*, in press. DOI: 10.1007/s10311-009-0208-z.
33 B. C. Faust and J. Hoigné, Sensitized photooxidation of phenols by fulvic acid and in natural waters, *Environ. Sci. Technol.*, 1987, **21**, 957-964.
34 P. G. Tratnyek and J. Hoigné, Photo-oxidation of 2,4,6-trimethylphenol in aqueous laboratory solutions and natural waters: kinetics of reaction with singlet oxygen, *J. Photochem. Photobiol., A*, 1994, **84**, 153-160.
35 J.-P. Aguer, D. Tétégan and C. Richard, Humic substances mediated phototrensformation of 2,4,6-trimethylphenol: a catalytic reaction, *Photochem. Photobiol. Sci.*, 2005, **4**, 451-453.
36 M. Czaplicka, Photo-degradation of chlorophenols in the aqueous solution, *J. Haz. Mat.*, 2006, **B134**, 45-59.
37 F. Javier Benitez, F. J. Real, J. L. Acero and C. Garcia, Kinetics of the transformation of phenyl-urea herbicides during ozonation of natural waters: Rate constants and model predictions, *Wat. Res.*, 2007, **41**, 4073-4084.
38 S. Canonica, B. Hellrung, P. Müller and J. Wirz, Aqueous oxidation of phenylurea herbicides by triplet aromatic ketones, *Environ. Sci. Technol*,. 2006, **40**, 6636-6641.
39 A. L. Boreen, B. L. Edhlund, J. B. Cotner and K. McNeill, Indirect photodegradation of dissolved free amino acids: the contribution of singlet oxygen nd the differential reactivity of DOM from various sources, *Environ. Sci. Technol*,. 2008, **42**, 5492-5498.
40 D. Vione, V. Maurino, C. Minero, M. E. Carlotti, S. Chiron and S. Barbati, Modelling the occurrence and reactivity of the carbonate radical in surface freshwater, *C. R. Chimie*, 2009, **12**, 865-871.
41 S. Chiron, C. Minero and D. Vione, Occurrence of 2,3-dichlorophenol and of 2,4-dichloro-6-nitrophenol in the Rhône River Delta (Southern France), *Environ. Sci. Technol.*, 2007, **41**, 3127-3133.
42 D. Vione, C. Minero, F. Housari and S. Chiron, Photoinduced transformation processes of 2,4-dichlorophenol and 2,6-dichlorophenol on nitrate irradiation, *Chemosphere*, 2007, **69**, 1548-1554.
43 S. Chiron, L. Comoretto, E. Rinaldi, V. Maurino, C. Minero and D. Vione, Pesticide by-products in the Rhône delta (Southern France). The case of 4-chloro-2-methylphenol and of its nitroderivative, *Chemosphere*, 2009, **74**, 599-604.
44 G. Grabner, C. Richard and G. Kohler, Formation and reactivity of 4-oxocyclohexa-2,5-dienyldiene in the photolysis of 4-chlorophenol in aqueous solution at ambient temperature, *J. Am. Chem. Soc.*, 1994, **116**, 11470-11480.